Contributions to Mineralogy and Petrology (2021) 176:47
https://doi.org/10.1007/s00410-021-01798-1

ORIGINAL PAPER

Immiscible silicate liquids: K and Fe distribution as a test for chemical equilibrium and insight into the kinetics of magma unmixing

Alexander Borisov[1] · **Ilya V. Veksler**[2,3]

Received: 6 December 2020 / Accepted: 28 April 2021 / Published online: 24 May 2021

Abstract

Silicate liquid immiscibility leading to formation of mixtures of distinct iron-rich and silica-rich liquids is common in basaltic and andesitic magmas at advanced stages of magma evolution. Experimental modeling of the immiscibility has been hampered by kinetic problems and attainment of chemical equilibrium between immiscible liquids in some experimental studies has been questioned. On the basis of symmetric regular solutions model and regression analysis of experimental data on compositions of immiscible liquid pairs, we show that liquid–liquid distribution of network-modifying elements K and Fe is linked to the distribution of network-forming oxides SiO_2, Al_2O_3 and P_2O_5 by equation: $\log K_{\mathrm{d}}^{\mathrm{K/Fe}} = 3.796\Delta X_{\mathrm{SiO_2}}^{\mathrm{sf}} + 4.85\Delta X_{\mathrm{Al_2O_3}}^{\mathrm{sf}} + 7.235\Delta X_{\mathrm{P_2O_5}}^{\mathrm{sf}} - 0.108$,where $K_{\mathrm{d}}^{\mathrm{K/Fe}}$ is a ratio of K and Fe mole fractions in the silica-rich (*s*) and Fe-rich (*f*) immiscible liquids: $K_d^{\mathrm{K/Fe}} = \left(X_{\mathrm{K}}^s / X_{\mathrm{K}}^f\right) / \left(X_{\mathrm{Fe}}^s / X_{\mathrm{Fe}}^f\right)$ and $\Delta X_{\mathrm{i}}^{sf}$ is a difference in mole fractions of a network-forming oxide *i* between the liquids (s) and (f): $\Delta X_i^{sf} = X_i^s - X_i^f$. We use the equation for testing chemical equilibrium in experiments not included in the regression analysis and compositions of natural immiscible melts found as glasses in volcanic rocks. Departures from equilibrium that the test revealed in crystal-rich multiphase experimental products and in natural volcanic rocks imply kinetic competition between liquid–liquid and crystal–liquid element partitioning. Immiscible liquid droplets in volcanic rocks appear to evolve along a metastable trend due to rapid crystallization. Immiscible liquids may be closer to chemical equilibrium in large intrusions where cooling rates are lower and crystals may be spatially separated from liquids.

Keywords Experimental petrology · Igneous rocks · Silicate melts · Liquid–liquid element distribution · Symmetric regular solutions

Introduction

Formation of immiscible mafic and felsic liquids is a common phenomenon in basaltic and andesitic magmas at advanced stages of crystallization (Thompson et al. 2007; Veksler and Charlier 2015 and references therein). Silicate liquid immiscibility is a peculiar case of phase separation, in which immiscible liquids do not dramatically differ in the types of chemical bonds, show significant mutual solubility and have very low values of interfacial tension (Veksler et al. 2010). In all these respects, immiscible silicate melts are distinct from other examples of immiscible liquid assemblages such as molten metals *vs*. slags, silicate *vs*. sulfide and carbonate magmatic melts or water *vs*. organic oils. There has been a growing concern in recent years that correct experimental reproduction of stable silicate immiscibility in multicomponent aluminosilicate

Communicated by Timothy L. Grove.

✉ Ilya V. Veksler
veksler@gfz-potsdam.de

Alexander Borisov
aborisov@igem.ru

[1] Institute of Geology of Ore Deposits, Petrography, Mineralogy and Geochemistry, Russian Academy of Sciences, Staromonetny 35, 109017 Moscow, Russia

[2] GFZ German Research Centre for Geosciences, Telegrafenberg, 14473 Potsdam, Germany

[3] V.S. Sobolev Institute of Geology and Mineralogy SB RAS, Akad. Koptyuga, 3, Novosibirsk 630090, Russia

compositions may be seriously hampered by kinetic obstacles and metastability (McBirney 2008; Morse 2008; Philpotts 2008; Veksler et al. 2008a, 2008b; Veksler and Charlier 2015). In view of the previously expressed doubts and disagreements, a practical means for testing chemical equilibrium between immiscible silicate melts would be helpful. Here, we propose a criterion for equilibrium based on liquid–liquid distribution of K and Fe, major elements of natural magmas showing the most contrasting distribution between immiscible silicate liquids. Thermodynamic aspects of the distribution are theoretically discussed in the frame of the symmetric regular solution model and the equilibrium constant is empirically calibrated against an extensive body of experimental data. We also discuss some applications to compositions of immiscible glasses in natural volcanic rocks and experimental products not included in the calibration.

Equilibrium crystal–liquid distribution of major components has been empirically calibrated for a number of important minerals and used in igneous petrology for equilibrium tests since long ago, e.g., Fe–Mg distribution between olivine and melt (Roeder and Emslie 1970). Notably, even the well-defined olivine-melt K_d^{FeMg} has been revisited and refined up till now in numerous studies (e.g., Toplis 2005; Blundy et al. 2020 and references therein). In contrast to crystals, conjugate compositions of multicomponent immiscible liquids lack the strict control from stoichiometry and are much more flexible. Nevertheless, one would expect some correspondence or correlation between the liquid–liquid distribution of network-modifying cations, such as K and Fe^{2+}, and network-forming components, such as silica and alumina. The likelihood of such correlation follows from the very nature of immiscibility, which is the ultimate consequence of non-ideality and strong coulombic interactions at the inter-ionic level (Hudon and Baker 2002). This study demonstrates that equilibrium relationship between liquid–liquid distribution of network-modifying and network-forming components does exist and has been reached in many (but not all) the experiments.

There are good reasons to expect nucleation of immiscible liquid droplets in multicomponent systems to happen faster than complete chemical equilibration between the liquid phases. Because diffusion rates of network-forming and network-modifying cations usually differ by orders of magnitude (Zhang et al. 2010), chemical equilibration between multicomponent immiscible melts may go through a series of metastable states and the true equilibrium distribution of all the components could be finally reached long after the initial unmixing. This study shows that metastable compositions of immiscible melts are especially common in experimental products and natural rocks with a large volume fraction of crystal phases.

Experimental data set

For the purpose of this study, we need melt compositions with a certain level of compositional complexity, which means more than one network former and more than one network modifier. Therefore, numerous binary oxide systems with stable silicate liquid immiscibility (Greig 1927; Hudon and Baker 2002) are not considered here but the synthetic five-component K_2O–FeO–Fe_2O_3–Al_2O_3–SiO_2 system with two network modifiers (K and ferrous iron) and three network formers, two of which (Al and ferric iron), according to classification by Hudon and Baker (2002), are amphoteric, meets the requirement. The system is the first and the best studied example of stable low-temperature immiscibility in complex aluminosilicate liquids (Roedder 1951) and chemical compositions of the immiscible Fe-rich and Si-rich liquids have been published in numerous papers (Bogaerts and Schmidt 2006; Freestone and Powell 1983; Kyser et al. 1998; Naslund 1983; Naslund and Watson 1977; Roedder and Weiblen 1970; Ryerson and Hess 1978; Vicenzi et al. 1994; Visser and Koster van Groos 1979a, b, c; Watson 1976). Liquids produced in these experiments were mostly above liquidus, but some experimental products contained minor amounts of crystal phases. We collected all the analyses of the conjugate liquid pairs from the above-cited publications, including compositions containing additional components, such as CaO, MgO and P_2O_5, and several nature-like multicomponent compositions with volatile components F and H_2O, and degree of crystallization less than 25 vol.% (Hou et al. 2017). The compiled dataset (see the Supplementary data file) includes 195 samples covering the temperature interval of 987–1540 °C, pressure from atmospheric to 1.5 GPa and the oxygen fugacity from air to that of below the iron-wüstite (IW) buffer.

The liquid–liquid distribution of K and Fe

Nernst distribution coefficients are the simplest conventional form of quantitative presentation of element partitioning between phases. In our case of liquid–liquid element partitioning, Nernst distribution coefficient of element A (D^A) between silica-rich (s) and Fe-rich (f) immiscible liquids is calculated as a ratio $D^A = C^s_A/C^f_A$, where C^s_A and C^f_A are mass concentrations of the element A in liquids s and f, respectively. It has been noted since long ago (Warren and Pincus 1940) that the liquid–liquid D values of network-modifying cations systematically change with ionic potential Z/r where Z is a nominal charge of the cation and r is its ionic radius. The dependence of D on Z/r is hardly surprising in view that Coulombic repulsion

between the cations appear to be the principal driving force for silicate liquid immiscibility at the atomic level (Hudon and Baker, 2002). In terms of the liquid–liquid distribution, K and Fe occupy the extreme positions among a dozen or so elements whose oxides are usually listed as major components in chemical analyses of igneous rocks. Ionic potential of K^+ is the lowest among the elements and K_2O is the major oxide most miscible with silica as there are no signs of stable or metastable immiscibility in the K_2O–SiO_2 binary system (Levin et al. 1964). In contrast, Fe^{2+} belongs to cations of variable crystal field stabilization energies (VCFSE) that have anomalously poor (relative to their *Z/r* characteristics) miscibility with silica in binary and multicomponent melts (Hudon and Baker, 2002). Therefore, liquid–liquid D^{Fe} values are the lowest and D^K are the highest among the major network-modifying elements of igneous rocks (Schmidt et al. 2006; Veksler et al. 2006).

The distribution coefficients are not the only conventional measure of compositional contrast between the immiscible liquids. It is a common practice in silicate systems to present the width of miscibility gap by the difference in silica concentrations $\Delta C_{SiO_2} = C^s_{SiO_2} - C^f_{SiO_2}$ expressed in weight percent. Silica is the main network-forming component of natural magmas and using ΔC_{SiO_2} is more convenient than using D^{Si}.

In Fig. 1, the *D* values of K and Fe are plotted in the logarithmic scale against ΔC_{SiO_2} for the experimental data

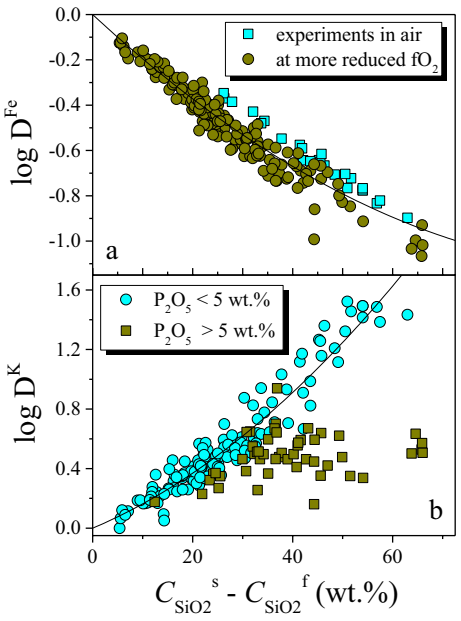

Fig. 1 Nernst liquid–liquid partition coefficients of Fe (**a**) and K (**b**) plotted against the difference in SiO_2 contents between the silica-rich and silica-poor immiscible liquids (wt.%)

described in the previous section. Regression analysis of the data shows that the log D^{Fe} values closely follow a quadratic polynomial curve

$$\log D^{Fe} = -2.04 \cdot 10^{-2} \cdot \Delta C_{SiO_2} + 9.23 \cdot 10^{-5} \cdot \left(\Delta C_{SiO_2}\right)^2 \quad (1)$$

implying that silica is the most important network-forming component controlling the distribution of Fe. It should be noted that the D^{Fe} values plotted in Fig. 1a are calculated for to the total Fe combining ferrous and ferric iron, and the two oxidation forms have very different chemical properties and structural roles in silicate melts. A moderate effect of Fe oxidation state does show up in Fig. 1a. Experiments conducted in air with predominantly ferric iron in both melts, (e.g., Borisov et al. 2018) plot slightly above other experiments the majority of which was carried out at very reducing conditions corresponding to those of the IW and Mo/MoO_2 buffers, when ferrous iron prevails. However, the apparent effect of oxidation on iron distribution is not great. A somewhat more contrasting liquid–liquid distribution of ferrous iron may be due to the above-mentioned anomalously poor miscibility of FeO with silica and the amphoteric role of Fe_2O_3 in silicate melts that should make ferric iron more compatible with silica network (Hudon and Baker 2002).

The situation with the $D^K - \Delta C_{SiO_2}$ correlation appears to be more complicated. Immiscible liquid pairs with $C^s_{P_2O_5} < 5$wt.% plot close to a polynomial curve

$$\log D^K = 1.23 \cdot 10^{-2} \cdot \Delta C_{SiO_2} + 2.35 \cdot 10^{-4} \cdot \left(\Delta C_{SiO_2}\right)^2. \quad (2)$$

However, P-rich compositions with $C^s_{P_2O_5} > 5$ wt.% systematically plot below the curve (2), implying that phosphorus, in addition to silica, has a strong effect on K distribution. The effect may be due to the formation of K-phosphate and Al-O-P species in the conjugate melts (Mysen et al. 1981; Toplis and Dingwell 1996). Regardless, the exact mechanism of interaction, the example of K clearly shows that network-forming components other than silica can strongly affect the liquid–liquid distribution of network-modifying cations and should not be excluded from consideration.

We should point out that the free terms in polynomials (1) and (2) were assumed to be 0, because at $\Delta C_{SiO_2} = 0$ (no phase separation and compositional contrast between liquid fractions) the D^K and D^{Fe} should be equal to 1, and the logarithms should be consequently at 0. If the regression is done without restrictions on the free term, the values of the free terms are indeed insignificant: -0.013 ± 0.02 (1 σ) in the polynomial (1) and 0.002 ± 0.04 in the polynomial (2).

Clearly, a more complex equation form should be found for better fitting the K and Fe partitioning both in P-poor

and P-rich systems. A logical next step would be to use a combined distribution coefficient $K_d^{K/Fe}$ defined as

$$K_d^{K/Fe} = \left(X_K^s / X_K^f\right) \Big/ \left(X_{Fe}^s / X_{Fe}^f\right), \quad (3)$$

where X_i^s and X_i^f are K or Fe mole fractions in silica-rich and Fe-rich liquids, correspondently. Using $K_d^{K/Fe}$ instead of D^K and D^{Fe} has a few advantages. First of all, K_d compensates, to some extent, possible systematic errors of microprobe analysis of K and Fe contents in immiscible liquids. But more importantly, thermodynamic description of K_d as shown below is simpler than those of D^K or D^{Fe}.

Thermodynamic analysis

In case, Fe-rich (*f*) and silica-rich (*s*) liquids are in equilibrium, any component, for example K_2O, is distributed according to equation:

$$K_2O\,(f) = K_2O\,(s), \quad (4)$$

with a constant of the reaction:

$$K_4 = a^s_{K_2O}/a^f_{K_2O} = \left(X^s_{K_2O}/X^f_{K_2O}\right)\cdot\left(\gamma^s_{K_2O}/\gamma^f_{K_2O}\right) = D^{sf}_K\cdot\left(\gamma^s_{K_2O}/\gamma^f_{K_2O}\right), \quad (5)$$

where $a^i_{K_2O}$, $X^i_{K_2O}$ and $\gamma^i_{K_2O}$ are activity, mole fraction and activity coefficient of K_2O in appropriate liquid and D_K is molar *K* distribution coefficient between silica-rich and Fe-rich melts. It is also valid that:

$$RT\cdot\ln K_4 = RT\cdot\ln D_K + RT\cdot\ln\left(\gamma^s_{K_2O}/\gamma^f_{K_2O}\right) = -\Delta G_K = -\Delta H_K + T\Delta S_K, \quad (6)$$

where ΔG_K, ΔH_K and ΔS_K are Gibbs free energy, enthalpy and entropy of reaction (4) and *T* is absolute temperature. The Eq. (6) may be further converted into:

$$RT\cdot\ln D_K = -\Delta H_K + T\Delta S_K - RT\cdot\ln\left(\gamma^s_{K_2O}/\gamma^f_{K_2O}\right). \quad (7)$$

A similar expression may be written for FeO partitioning between Fe-rich and silica-rich liquids:

$$RT\cdot\ln D_{Fe} = -\Delta H_{Fe} + T\Delta S_{Fe} - RT\cdot\ln\left(\gamma^s_{FeO}/\gamma^f_{FeO}\right). \quad (8)$$

Subtracting (8) from (7), one can define the K-Fe partition coefficient:

$$RT\cdot\ln K_d^{K/Fe} = -\left(\Delta H_K - \Delta H_{Fe}\right) + T\left(\Delta S_K - \Delta S_{Fe}\right) - RT\cdot\ln\left(\gamma^s_{K_2O}/\gamma^f_{K_2O}\right)\Big/\left(\gamma^s_{FeO}/\gamma^f_{FeO}\right). \quad (9)$$

Let us now consider the form of expression for the activity coefficients. For simplicity and clarity, let us examine quaternary solutions (e.g., SiO_2–Al_2O_3–FeO–K_2O) and restrict the analysis to symmetric regular solutions (all the definitions and primary formulae are according to Mukhopadhyay et al, 1993). The activity coefficients of K_2O in two coexisting liquids are defined as:

$$RT\cdot\ln\gamma^s_{K_2O} = X^s_{FeO}W_{K\text{-}Fe} + X^s_{Al_2O_3}W_{K\text{-}Al} + X^s_{SiO_2}W_{K\text{-}Si} - G^s_{ex} \quad (10)$$

$$RT\cdot\ln\gamma^f_{K_2O} = X^f_{FeO}W_{K\text{-}Fe} + X^f_{Al_2O_3}W_{K\text{-}Al} + X^f_{SiO_2}W_{K\text{-}Si} - G^f_{ex}, \quad (11)$$

where R is the gas constant, W_{ij} are interaction parameters and G_{ex} are excess free energies in the silica-rich and iron-rich liquids. Subtraction (11) from (10) gives:

$$RT\cdot\ln\left(\gamma^s_{K_2O}/\gamma^f_{K_2O}\right) = \left(X^s_{FeO} - X^f_{FeO}\right)W_{K\text{-}Fe} + \left(X^s_{Al_2O_3} - X^f_{Al_2O_3}\right)W_{K\text{-}Al} + \left(X^s_{SiO_2} - X^f_{SiO_2}\right)W_{K\text{-}Si} - \left(G^s_{ex} - G^f_{ex}\right), \quad (12)$$

or

$$RT\cdot\ln\left(\gamma^s_{K_2O}/\gamma^f_{K_2O}\right) = \Delta X^{sf}_{FeO}W_{K\text{-}Fe} + \Delta X^{sf}_{Al_2O_3}W_{K\text{-}Al} + \Delta X^{sf}_{SiO_2}W_{K\text{-}Si} - \Delta\left(G_{ex}\right)^{sf}, \quad (13)$$

where ΔX_i^{sf} is a difference of the mole fractions of a component i between silica-rich and Fe-rich liquids and ΔG_{ex} is a difference in the excess free energies. A similar expression can be written for FeO activity coefficients:

$$RT\cdot\ln\left(\gamma^s_{FeO}/\gamma^f_{FeO}\right) = \Delta X^{sf}_{K_2O}W_{K\text{-}Fe} + \Delta X^{sf}_{Al_2O_3}W_{K\text{-}Al} + \Delta X^{sf}_{SiO_2}W_{Fe\text{-}Si} - \Delta\left(G_{ex}\right)^{sf}. \quad (14)$$

Subtracting (14) from (13) and keeping in mind that $W_{K\text{-}Fe} = W_{Fe\text{-}K}$ in the symmetric regular model, we get:

$$RT\cdot\ln\left(\gamma^s_{K_2O}/\gamma^f_{K_2O}\right)\Big/\left(\gamma^s_{FeO}/\gamma^f_{FeO}\right) = \left(\Delta X^{sf}_{FeO} - \Delta X^{sf}_{K_2O}\right)W_{K\text{-}Fe} + \Delta X^{sf}_{Al_2O_3}\left(W_{K\text{-}Al}/W_{Fe\text{-}Al}\right) + \Delta X^{sf}_{SiO_2}\left(W_{K\text{-}Si}/W_{Fe\text{-}Si}\right). \quad (15)$$

Substituting (15) in (9) gives:

$$RT \cdot \ln K_d^{KFe} = -\left(\Delta H_K - \Delta H_{Fe}\right) + T\left(\Delta S_K - \Delta S_{Fe}\right) - \left(\Delta X_{FeO}^{sf} - \Delta X_{K_2O}^{sf}\right) W_{K\text{-}Fe} - \Delta X_{Al_2O_3}^{sf}\left(W_{K\text{-}Al} - W_{Fe\text{-}Al}\right) - \Delta X_{SiO_2}^{sf}\left(W_{K\text{-}Si} - W_{Fe\text{-}Si}\right). \quad (16)$$

Dividing both sides of (16) by RT, changing natural logarithms (ln) to the common ones (log) and generalizing the expression, one can expect an equation in the form of

$$\log K_d^{K/Fe} = h/T + \sum a_i \Delta X_i^{sf}/T + b\left(\Delta X_{FeO}^{sf} - \Delta X_{K_2O}^{sf}\right)/T + c, \quad (17)$$

where h, a_i, b and c = const, and in the sum the term i ≠ K or Fe. In this equation, the temperature slope $h = -(\Delta H_K - \Delta H_{Fe})/2.303R$, $a_i = -(W_{K\text{-}I} - W_{Fe\text{-}i})/2.303R$, $b = -W_{K\text{-}Fe}/2.303R$, and $c = (\Delta S_K - \Delta S_{Fe})/2.303R$. The form of the Eq. (17) is relatively simple. As mentioned above, using $K_d^{K/Fe}$ is practical, because G_{ex} terms are canceled out. The parameter h may be expected to be small or even close to zero, if $\Delta H_K \approx \Delta H_{Fe}$.

Proceeding with asymmetric regular solutions would have extremely complicated the equation with additional terms $X_i X_j$, X_i^2 and $X_i X_j^2$, and we will not consider it here. Instead, in addition to (17), we would also consider equations in the form:

$$\log K_d^{K/Fe} = h/T + \sum a_i \Delta X_i^{sf} + b\left(\Delta X_{FeO}^{sf} - \Delta X_{K_2O}^{sf}\right) + c, \quad (18)$$

where h, a_i, b and c = const, and in the sum the term i ≠ K or Fe. When describing a partition coefficient as a function of the melt composition, it may be useful to check if mole fractions of oxides in the melt as entropy-like terms (not divided by temperature) give a better fit than enthalpy-like terms (divided by temperature) (Mallmann and O'Neill 2013).

At first, the selected dataset (see above) was fitted with multiple linear regressions using all possible terms in Eq. (17) and (18). It was found that model (18) is typically slightly better than model (17). Then, by trial and error, we removed one term after another trying to minimize the number of variables without compromising the accuracy (R^2) too much. Three experiments from the dataset with standardized residuals typically exceeding 3.5σ in most models were removed and the final equations are based on 192 experiments (see the Supplementary file). In the dataset used for calibration, the value of $K_d^{K/Fe}$ lies in the range from 1.33 to 214 and may be precisely ($R^2 = 0.974$) fitted with the form (18) equation containing only $\Delta X_{SiO_2}^{sf}$, $\Delta X_{Al_2O_3}^{sf}$, $\Delta X_{P_2O_5}^{sf}$, 1/T and a free term:

$$\log K_d^{K/Fe} = 818.5/T + 4.065\,\Delta X_{SiO_2}^{sf} + 3.386\,\Delta X_{Al_2O_3}^{sf} + 7.550\,\Delta X_{P_2O_5}^{sf} - 0.707. \quad (19)$$

As expected, the temperature slope $h = 818.5 \pm 152.6$ is rather shallow and defined with a relatively large error. Thus, one can exclude the temperature term h/T and, with an insignificant loss of accuracy ($R^2 = 0.970$), obtain the following expression:

$$\log K_d^{K/Fe} = 3.796\,\Delta X_{SiO_2}^{sf} + 4.85\,\Delta X_{Al_2O_3}^{sf} + 7.235\,\Delta X_{P_2O_5}^{sf} - 0.108. \quad (20)$$

Equation (20) is especially useful for applications to immiscibility in natural rocks, because it does not require any assumptions regarding the temperature. Free terms c in the equations are not large but we decided not to set them to zero (as explained above for Eq. 1 and 2), since c may accumulate all possible errors of the model which ignores the effects of all the components other than silica, alumina and P_2O_5. The empirical coefficients at ΔX_i^{sf} in Eqs. (19) and (20) are defined with high accuracy (see Table 1) and they imply that the effects of these components on the value of $\log K_d^{K/Fe}$ are in the order $SiO_2 \le Al_2O_3 << P_2O_5$.

In Fig. 2, we compare experimental K_d values that are directly derived from the measured concentrations of K and Fe in the conjugate liquids using Eq. (3) with K_d values calculated from the measured concentrations of Si, Al and P using the empirically calibrated model [Eq. (20)]. The comparison shows that Eq. (20) works equally well at pressures from atmospheric to 1.5 GPa (Fig. 2a), high-temperature and low-temperature experiments (Fig. 2b), highly oxidizing and

Table 1 Coefficients and other statistical information for model equations in the form $\log K_d^{K/Fe} = h/T + a\Delta X_{Al_2O_3}^{sf} + c\Delta X_{P_2O_5}^{sf} + d$

	Equation (19)		Equation (20)	
	Value	St. error	Value	St. error
h	818.5	152.6	–	–
a	4.065	0.070	152.6	0.053
b	3.386	0.561	4.85	0.525
c	7.55	0.225	7.235	0.233
d	− 0.707	0.113	− 0.108	0.016
R^2	0.974		0.970	
St. error	0.075		0.081	
Observations	192		192	

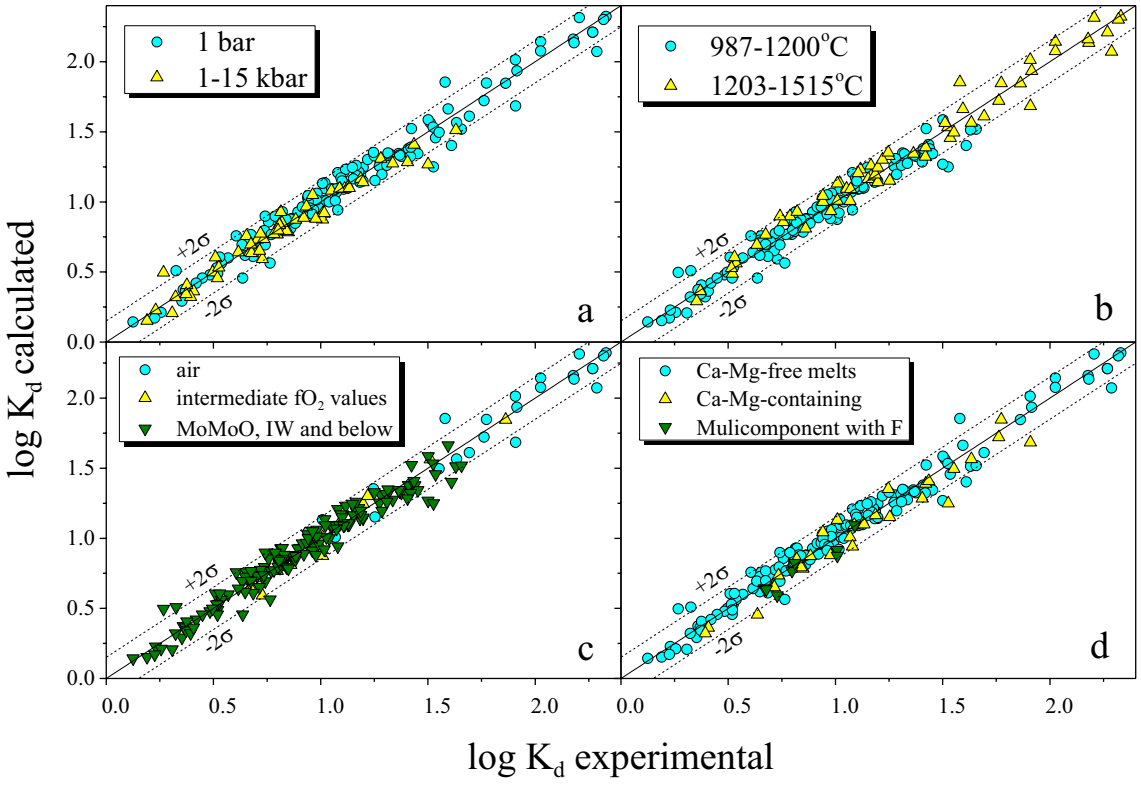

Fig. 2 Expected values of $K_d^{K/Fe}$ according to Eq. (20) versus measured values based on direct analyses of K and Fe (Eq. 3). Data points are sorted by pressure (**a**), temperature (**b**), oxygen fugacity (**c**) and the melt composition (**d**). Neither of the parameters show any systematic effects

reducing conditions (Fig. 2c), and for simplified five-oxide and multicomponent compositions (Fig. 2d). Therefore, it appears that plotting measured $K_d^{K/Fe}$ values obtained using Eq. (3) against expected from Eq. (20), or Eq. (19) if equilibration temperature is known, can be used for testing the approach to equilibrium and the quality of chemical analyses for immiscible silicate liquids of variable compositions containing both K and Fe oxides over a broad range of pressures and temperatures.

Applications

Let us now apply the equilibrium test to experimental products that were not included in calibration of Eqs. (19) and (20) and also to published analyses of natural immiscible silicate liquids that have been found as quenched glasses in volcanic rocks.

Centrifuge and reverse experiments

Experiments by Veksler et al. (2006, 2007, 2008a) employed high-temperature centrifugation and were excluded from the

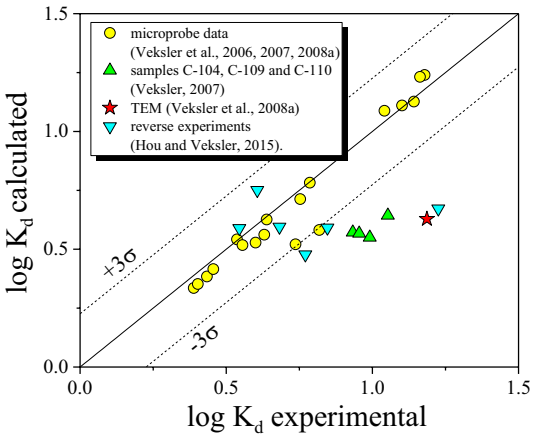

Fig. 3 Equilibrium test for immiscible liquids produced in centrifugation and reverse experiments. Yellow circles: electron microprobe data from Veksler et al. (2006, 2007, 2008a). Green triangles: silicate liquids associated with the third immiscible liquid of Fe phosphide composition (Veksler 2007, samples C-104, C-109 and C-110). Red star: semi-quantitative TEM analyses of sub-micron emulsions (Veksler et al. 2008a). Blue triangles: liquids from reverse experiments (Hou and Veksler 2015). See text for discussion

dataset that we used for calibrating the Eqs. (19) and (20). Some researches argued that fine emulsions produced in the experiments were metastable and had formed during quench. Disagreements regarding the nature and interpretation of the centrifugation products, and the maximal temperature of stable silicate liquid immiscibility in basaltic magma led to a public discussion (McBirney 2008; Morse 2008; Philpotts 2008; Veksler et al. 2008b) and inspired reverse experiments (Hou and Veksler 2015) that apparently confirmed stable, super-liquidus immiscibility in a few basaltic and andesitic compositions at 1150–1200 °C.

As demonstrated in Fig. 3, the majority of microprobe analyses of conjugate immiscible liquids published by Veksler et al. (2006, 2007, 2008a) show good agreement between the measured and expected K_d values, and typically plot within 1σ limits around the equilibrium line. Two experiments C-108 and C-114 in the system fayalite–anorthite–orthoclase–silica, which produced especially fine emulsion of one immiscible liquid in another (Veksler et al. 2008a), show a slightly higher mismatch between the K_d values. However, they are still mostly within the 3σ error limits. Semi-quantitative transmission electron microscopy (TEM) analyses of individual nanoscale droplets in sample C-108 apparently produced less accurate results with K_d values differing by 7.2σ. Four samples marked by green triangles, which are also out of the 2σ area, represent products of centrifuge experiments C-104, C-109 C-110 and C-112 from the study by Veksler et al. (2007). Those experiments were distinguished by the formation of a third immiscible liquid of an iron phosphide composition, probably due to reduction of the P_2O_5 component in silicate melts by carbon residing in steel containers. Separation of the reduced Fe–P liquid had a negligible effect on the FeO content of the silicate melts, but resulted in a significant drop of P_2O_5 concentrations in the Fe-rich silicate liquid. This apparently led to disequilibrium in P_2O_5 distribution between immiscible silicate liquids and, consequently, to the lower K_d values derived from Eq. (20).

Experiments on compositions with H_2O and other volatile components

Lester et al. (2013) studied the effects of H_2O alone and in combination with other volatile components (P, S, F and Cl) on silicate liquid immiscibility in the system K_2O–FeO–Fe_2O_3–Al_2O_3–SiO_2 at 200 MPa and redox conditions equivalent to those of the quartz–fayalite–magnetite (QFM), Ni–NiO and magnetite–hematite (MH) oxygen buffers. Experiments were carried out in rapid quench internally heated pressure vessels at 1075, 1150 at 1200 °C. The initial content of H_2O was kept at 10 wt.%,

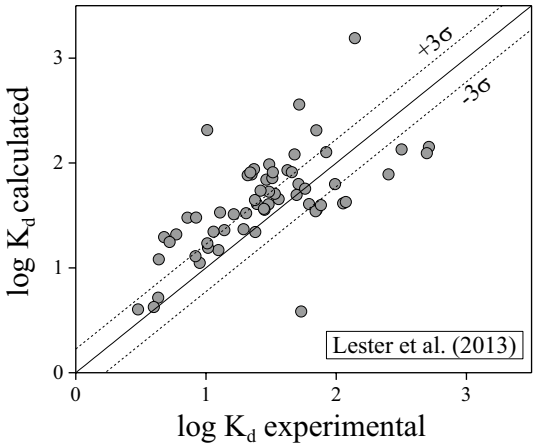

Fig. 4 Equilibrium test for immiscible liquids with volatile components (Lester et al. 2013) using Eq. (19). See text for discussion

the initial FeO content was at 30 wt.% and K/Al molar ratio at 1. All the experiments on H_2O-bearing compositions produced a vapor phase. Several experiments on starting compositions with 2 wt.% S produced a third immiscible Fe-sulfide liquid in addition to immiscible silicate melts. Some run products included one or two crystal phases identified as silica polymorphs and magnetite.

The results of equilibrium test for the compositions of immiscible silicate liquids produced in that study are presented in Fig. 4. We have used Eq. (19) but Eq. (20) gives a similar result. Most of the experiments show strong and random deviations from the equilibrium line. We were unable to find any systematic variations correlating with the added components, temperature, oxygen fugacity or phase composition of the run products. It is not clear why the results of the study flunk the equilibrium test. The reasons may include analytical problems, significant losses of some components to the vapor phase, Fe losses to platinum containers or insufficient equilibration time.

Experiments on crystal-rich compositions

As noted above, experimental products that we used for the calibration of Eqs. (19) and (20) were either super-liquidus glasses without any crystals or assemblages with small amounts of crystal phases, usually represented by magnetite and quartz. Experimental products with high proportion of crystals were excluded from the calibration. Those experiments were usually done on powders or chips of natural igneous rocks, and the examples that we compiled in our dataset (see the Supplementary data file) include chemical analyses from publications by Dixon and Rutherford (1979), Philpotts (1981), Philpotts and Doyle (1983), Longhi (1990), Tollari et al. (2006), Charlier and Grove (2012), Hou et al. (2018) and Honour et al. (2019a).

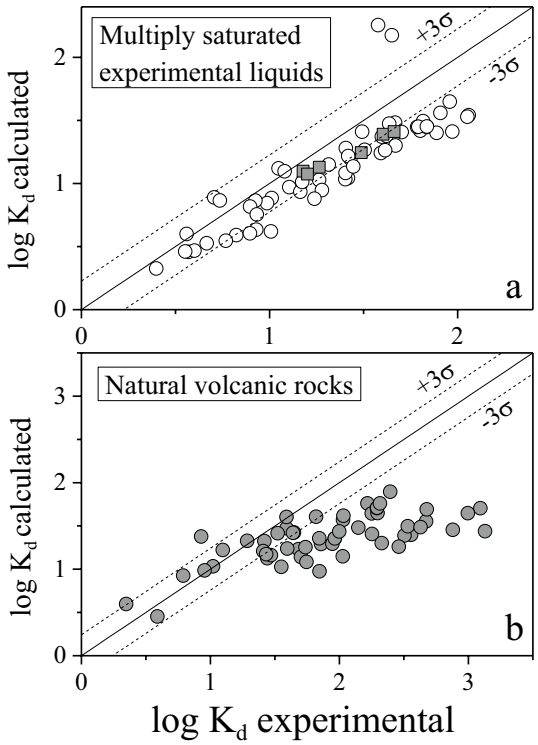

Fig. 5 Equilibrium test for immiscible liquids in highly crystallized experimental products (**a**) and natural samples of volcanic rocks (**b**). See text for details

The equilibrium test proposed here (Fig. 5a) shows that liquid pairs with less contrasting distribution of K and Fe (low K_d values) plot close to the equilibrium line, but as the conjugate liquids become chemically more distinct (higher K_d values), they tend to plot farther and farther to the right of equilibrium line. This tendency is best illustrated by products of two time series carried out by Honour et al. (2019a). Crushed rock of monzonitic composition from the Sept Iles intrusion (Quebec, Canada) was used as a starting material for the series of isothermal experiments at 1000 and 1021 °C. The products highlighted by gray squares in Fig. 5a show that while the exposure time increased from 115 to 306 h the compositions of the conjugate liquids became more contrasting but followed a trend with a shallower slope than that of the equilibrium line. Shift to the right from the equilibrium line is minor in the data published by Honour et al. (2019a) and may be insignificant as their points in Fig. 5a remain within the 3σ interval. However, many other experiments plot out of the ±3σ range and they are also mostly skewed to the right. Skewness to the right implies less contrasting distribution of network formers Si, Al and P that is not matching the observed distribution of network modifiers K and Fe. In our view, this trend is probably a consequence of kinetic competition between crystal growth and diffusion-limited transport of components between and within the immiscible liquids. Such interpretation is supported by microstructures that Honour et al. (2019a) and Philpotts (1981) observed on surfaces of plagioclase crystals in their experimental products and in natural igneous rocks. They noticed that in those places where droplets of immiscible Fe-rich liquid attached to faces of plagioclase laths, plagioclase crystals grew faster and developed pillar structures that protruded outward by about 2–5 μm. Notably, plagioclase pillars are more albitic than the rest of the crystal and the chemical divide is sharp (Honour et al. 2019a). It appears that for kinetic reasons droplets of Fe-rich liquid in direct contact with plagioclase tend to exsolve components more compatible with immiscible silica-rich liquid (Na, Al and Si) into a new plagioclase growth rather than to surrounding volume of the conjugate melt. Interplay between plagioclase crystallization and silicate liquid immiscibility is even more evident in natural magmas (see the next section).

Natural immiscible liquids

Similar disequilibrium in liquid–liquid element distribution, but of a much greater magnitude, is revealed in samples of natural volcanic rocks (Fig. 5b). Data plotted in Fig. 5b include samples of terrestrial and lunar basaltic and andesitic rocks (Charlier et al. 2013; Kamenetsky et al. 2013; Krasov and Clocciatti 1979; Pedersen 1985; Neal and Taylor 1989; Philpotts 1982; Philpotts and Doyle 1983; Roedder and Weiblen, 1971; Shearer et al. 2001) crystallized in vastly different geologic environments and redox conditions. Immiscible liquids in the rocks have been observed either as microscopic droplets of glasses dispersed in the groundmass between microcrysts of pyroxenes, plagioclase, Fe–Ti oxides and other minerals, or as glassy inclusions in olivine and plagioclase phenocrysts. Clearly, most of the natural immiscible liquids found in close association with silicate and oxide crystals are not in chemical equilibrium. Typically, K_d values based on the measured concentrations of K and Fe (Eq. 3) are 2–5 times greater than the expected values derived from Eq. (20), but in some cases, the difference is as much as 15 times. We believe that the mechanism behind disequilibrium proposed for crystal-rich experimental products in the previous section is even more likely to operate in natural volcanic systems where no deliberate human efforts have been made for reaching proper equilibrium.

According to the model developed by Giordano et al. (2008), viscosity of a typical Si-rich immiscible liquid from natural basaltic rocks (Philpotts 1982) at 1050 °C is 3.5 log-units, or 3200 times, greater than the viscosity of Fe-rich liquid, and the glass transition temperature of the Si-rich liquid is by 80 °C higher than that of the Fe-rich liquid (780 vs. 700 °C). This implies that material transport by diffusion and crystal growth in the Fe-rich liquid should be much faster, and continue for a longer period of time down

to lower temperatures than in the Si-rich liquid phase. In this situation, chemical equilibration between crystals and Fe-rich liquid may kinetically out-compete liquid–liquid equilibration and result in metastable, disequilibrium distribution of network formers and network modifiers. Strong empirical support for this proposition has been recently provided by Honour et al. (2019b). They observed that continuous films of Fe-rich liquid with distinct interfaces had formed in compositional boundary layers (CBL) around plagioclase crystals growing in basaltic lava of Kilauea Iki lava lake. Similar films of Si-rich liquid were observed in CBL around clinopyroxene in the same samples. The observations show that one of immiscible silicate liquids may nucleate alone, without a second conjugate liquid phase if all the main components of the latter are incorporated by adjacent growing crystals. Clearly, this is an extreme case of metastability caused by kinetic competition between crystallization and liquid immiscibility.

The situation may be, however, different in large intrusive bodies of magma where cooling rates are lower and crystals may be spatially separated from liquids. Immiscible liquids in plutonic systems may have enough time for attaining equilibrium distribution of all the components. However, those liquids have never been sampled directly. In large plutonic systems, we are dealing only with completely crystallized rocks where traces of liquid immiscibility have been preserved only in crystal microstructures (Holness et al. 2011) or crystallized melt inclusions (Jakobsen et al. 2005, 2011).

Concluding remarks

The results of equilibrium tests presented here highlight experimental challenges posed by silicate liquid immiscibility. They arise to a large extent from complex kinetic relationships between liquid–liquid and crystal–liquid chemical interactions and vastly different diffusion rates of network-forming and network-modifying cations in the conjugate liquids. Conventional experiments on small, millimeter-sized samples with high volume fractions of crystals may not correctly reproduce equilibrium compositions of immiscible liquids despite very long exposure times. Compositions of microscopic immiscible liquid droplets in crystalline matrix of volcanic rocks appear to evolve along a metastable trend and may differ from immiscible liquids in plutonic products of the same magma. In view of experimental difficulties and kinetic effects in volcanic rocks accessible for direct observations, the extent and petrogenetic role of silicate liquid immiscibility in plutonic systems may be underestimated and deserve a revision.

Supplementary Information The online version contains supplementary material available at https://doi.org/10.1007/s00410-021-01798-1.

Acknowledgements We greatly appreciate constructive and thoughtful comments from two anonymous reviewers that helped us to strengthen our arguments. IVV has been supported by Russian Science Foundation Grant No. 19-17-00013.

Funding Open Access funding enabled and organized by Projekt DEAL. Ilya Veksler is currently supported by DFG (Deutsche Forschungsemeinschaft) grant VE 619–6-1 and RSF (Russian Science Foundation) Grant No. 19-17-00013.

Data availability All the background information is presented in a supplementary data file.

Declarations

Conflict of interest None.

References

Blundy J, Melekhova E, Ziberna L, Humphreys MC, Cerantola V, Brooker RA, McCammon CA, Pichavant M, Ulmer P (2020) Effect of redox on Fe–Mg–Mn exchange between olivine and melt and an oxybarometer for basalts. Contrib Miner Pet 175:103

Bogaerts M, Schmidt MW (2006) Experiments on silicate melt immiscibility in the system Fe_2SiO_4–$KAlSi_3O_8$–SiO_2–CaO–MgO–TiO_2–P_2O_5 and implications for natural magmas. Contrib Miner Pet 152:257–274

Borisov A, Behrens H, Holtz F (2018) Ferric/ferrous ratio in silicate melts, a new model for 1 atm data with special emphasis on the effects of melt composition. Contrib Mineral Petrol 173, Article 98

Charlier B, Grove TL (2012) Experiments on liquid immiscibility along tholeiitic liquid lines of descent. Contrib Miner Pet 164:27–44

Charlier B, Namur O, Grove TL (2013) Compositional and kinetic controls on liquid immiscibility in ferrobasalt–rhyolite volcanic and plutonic series. Geochim Cosmochim Acta 113:79–93

Dixon S, Rutherford MJ (1979) Plagiogranites as late-stage immiscible liquids in ophiolite and mid-ocean ridge suites: an experimental study. Earth Planet Sci Lett 45:45–60

Freestone IC, Powell P (1983) The low temperature field of liquid immiscibility in the system K_2O-FeO-Al_2O_3-SiO_2 with special reference to the join fayalite-leucite-silica. Contrib Miner Pet 82:291–299

Giordano D, Russell JK, Dingwell DB (2008) Viscosity of magmatic liquids: a model. Earth Planet Sci Lett 271:123–134

Greig JW (1927) Immiscibility in silicate melts. Amer J Sci 13:133–154

Holness MB, Stripp G, Humphreys MCS, Veksler IV, Nielsen TFD (2011) Silicate liquid immiscibility within the crystal mush: late-stage magmatic microstructures in the Skaergaard intrusion, East Greenland. J Petrol 52:175–222

Honour VC, Holness MB, Partridge JL, Charlier B (2019a) Microstructural evolution of silicate immiscible liquids in ferrobasalts. Contrib Miner Pet 174(9):77

Honour VC, Holness MB, Charlier B, Piazolo SC, Namur O, Prosa TJ, Martin I, Helz RT, Jean MJ, MM, (2019b) Compositional boundary layers trigger liquid unmixing in a basaltic crystal mush. Nature Comm 10(1):1–8

Hou T, Veksler IV (2015) Experimental confirmation of high-temperature silicate liquid immiscibility in multicomponent ferrobasaltic systems. Amer Miner 100:1304–1307

Hou T, Charlier B, Namur O, Schütte P, Schwarz-Schampera U, Zhang Z, Holtz F (2017) Experimental study of liquid immiscibility in the Kiruna-type Vergenoeg iron-fluorine deposit, South Africa. Geochim Cosmochim Acta 203:303–322

Hou T, Charlier B, Holtz F, Veksler I, Zhang Z, Thomas R, Namur O (2018) Immiscible hydrous Fe-Ca-P melt and the origin of iron oxide-apatite ore deposits. Nature Comm 9(1): 1–8. https://www.nature.com/articles/s41467-018-03761-4. Accessed 12 April 2018

Hudon P, Baker DR (2002) The nature of phase separation in binary oxide melts and glasses. I. Silicate systems. J Non-Cryst Solids 303:299–345

Jakobsen JK, Veksler IV, Tegner C, Brooks CK (2005) Immiscible iron- and silica-rich melts in basalt petrogenesis documented in the Skaergaard intrusion. Geology 33:885–888

Jakobsen JK, Veksler IV, Tegner C, Brooks CK (2011) Crystallization of the Skaergaard intrusion from an emulsion of immiscible iron- and silica-rich liquids: evidence from melt inclusions in plagioclase. J Pet 52:345–373

Kamenetsky VS, Charlier B, Zhitova L, Sharygin V, Davidson P, Feig S (2013) Magma chamber–scale liquid immiscibility in the Siberian traps represented by melt pools in native iron. Geology 41:1091–1094

Krasov NF, Clocchiatti R (1979) Immiscibility in silicate melts and its possible petrogenetic importance, as shown by study of melt inclusions (trans Doklady). USSR Acad Sci 248:92–95

Kyser TK, Lesher CE, Walker D (1998) The effects of liquid immiscibility and thermal diffusion on oxygen isotopes in silicate liquids. Contrib Miner Pet 133:373–381

Lester GW, Clark AH, Kyser TK, Naslund HR (2013) Experiments on liquid immiscibility in silicate melts with H_2O, P, S, F, and Cl: Implications for natural magmas. Contrib Miner Pet 166:329–349

Levin EM, Robbins CR, McMurdie HF (1964) Phase equilibria diagrams, vol 1. American Ceramic Society, Westerville

Longhi J (1990) Silicate liquid immiscibility in isothermal crystallization experiments. In: Lunar and planetary science conference proceedings, vol 20. Lunar and Planetary Institute, Houston, TX, pp 13–24

Mallmann G, O'Neill HC (2013) Calibration of an empirical thermometer and oxybarometer based on the partitioning of Sc, Y and V between olivine and silicate melt. J Pet 54:933–949

McBirney AR (2008) Comments on: 'liquid immiscibility and the evolution of basaltic magma' journal of petrology 48, 2187–2210. J Pet 49:2169–2170

Morse SA (2008) Compositional convection trumps silicate liquid immiscibilty in layered intrusions: a discussion of 'liquid immiscibility and the evolution of basaltic magma' by Veksler et al., journal of petrology 48, 2187–2210. J Pet 49:2157–2168

Mukhopadhyay B, Basu S, Holdaway MJ (1993) A discussion of Margules-type formulations for multicomponent solutions with a generalized approach. Geochim Cosmochim Acta 57:277–283

Mysen BO, Ryerson FJ, Virgo D (1981) The structural role of phosphorus in silicate melts. Amer Miner 66:106–117

Naslund HR (1983) The effect of oxygen fugacity on liquid immiscibility in iron-bearing silicate melts. Am J Sci 283:1034–1059

Naslund HR, Watson EB (1977) The effect of pressure on liquid immiscibility in the system K_2O-FeO-Al_2O_3-SiO_2-CO_2. Carnegie Inst Wash Year Book 76:410–414

Neal CR, Taylor LA (1989) The nature of Ba partitioning between immiscible melts: a comparison of experimental and natural systems with reference to lunar felsite petrogenesis. In: Lunar and planetary science conference, 19th, Houston, TX, Mar. 14–18, 1988, Proceedings (A89-36486 15-91). Cambridge/Houston, TX, Cambridge University Press/Lunar and Planetary Institute, 1989, pp 209–218

Pedersen AK (1985) Reaction between picrite magma and continental crust: tertiary silicic basalts and magnesian andesites from Disco West Greenland. Grønlands Geologiske Undersøgelse Bull (copenhagen) 152:126

Philpotts AR (1981) A model for the generation of massif-type anorthosites. Can Miner 19:233–253

Philpotts AR (1982) Compositions of immiscible liquids in volcanic rocks. Contrib Miner Pet 80:201–218

Philpotts AR (2008) Comments on: liquid immiscibility and the evolution of basaltic magma. J Pet 49:2171–2175

Philpotts AR, Doyle CD (1983) Effect of magma oxidation state on the extent of silicate liquid immiscibility in a tholeiitic basalt. Am J Sci 283(9):967–986

Roedder E (1951) Low-temperature liquid immiscibility in the system K_2O-FeO-Al_2O_3-SiO_2. Am Miner 36:282–286

Roedder E, Weiblen PW (1970) Lunar petrology of silicate melt inclusions, Apollo 11 rocks. Proc Apollo 11 Lun Sci Conf Geochim Cosmochim Acta 1(Suppl 1):507–528

Roedder E, Weiblen PW (1971) Petrology of silicate melt inclusions, Apollo 11 and Apollo 12 and terrestrial equivalents. Proc 2nd Lunar Sci Conf Geochim Cosmochim Acta 1(Suppl 2):507–528

Roeder PL, Emslie R (1970) Olivine-liquid equilibrium. Contrib Miner Pet 29:275–289

Ryerson FJ, Hess PC (1978) Implications of liquid-liquid distribution coefficients to mineral-liquid partitioning. Geochim Cosmochim Acta 42:921–932

Schmidt MW, Connolly JAD, Günther D, Bogaerts M (2006) Element partitioning—the role of melt structure and composition. Science 312:1646–1650

Shearer CK, Papike JJ, Spilde MN (2001) Trace element partitioning between immiscible lunar melts: an example from naturally occurring lunar melt inclusions. Amer Miner 86:238–241

Thompson AB, Aerts M, Hack AC (2007) Liquid immiscibility in silicate melts and related systems. In: Liebscher A, Heinrich CA (eds) Fluid-fluid interactions. Rev Mineral Geochem 65:99–127

Tollari N, Toplis MJ, Barnes S-J (2006) Predicting phosphate saturation in silicate magmas: an experimental study of the effects of melt composition and temperature. Geochim Cosmochim Acta 70(6):1518–1536

Toplis MJ (2005) The thermodynamics of iron and magnesium partitioning between olivine and liquid: criteria for assessing and predicting equilibrium in natural and experimental systems. Contrib Miner Pet 149:22–39

Toplis MJ, Dingwell DB (1996) The variable influence of P_2O_5 on the viscosity of melts of differing alkali/aluminium ratio: Implications for the structural role of phosphorus in silicate melts. Geochim Cosmochim Acta 60(21):4107–4121

Veksler IV, Charlier B (2015) Silicate liquid immiscibility in layered intrusions. In: Namur O, Latypov R, Tegner C (eds) Charlier B. Layered intrusions Springer, Dordrecht, pp 229–258

Veksler IV, Dorfman AM, Danyushevsky LM, Jakobsen JK, Dingwell DB (2006) Immiscible silicate liquid partition coefficients: implications for crystal-melt element partitioning and basalt petrogenesis. Contrib Miner Pet 152:685–702

Veksler IV, Dorfman AM, Borisov AA, Wirth R, Dingwell DB (2007) Liquid immiscibility and evolution of basaltic magma. J Pet 48:2187–2210

Veksler IV, Dorfman AM, Rhede D, Wirth R, Borisov AA, Dingwell DB (2008a) Liquid unmixing kinetics and the extent of immiscibility in the system K_2O–CaO–FeO–Al_2O_3–SiO_2. Chem Geol 256:119–130

Veksler I, Dorfman A, Borisov AA, Wirth R, Dingwell DB (2008b) Liquid immiscibility and evolution of basaltic magma: reply to S. A. Morse, A. R. McBirney and A R Philpotts. J Pet 49:2177–2186

Veksler IV, Kahn J, Franz G, Dingwell DB (2010) Interfacial tension between immiscible liquids in the system K_2O-FeO-Fe_2O_3-Al_2O_3-SiO_2 and implications for the kinetics of silicate melt unmixing. Amer Miner 95:1679–1685

Vicenzi E, Green T, Sie S (1994) Effect of oxygen fugacity on trace-element partitioning between immiscible silicate melts at atmospheric pressure: a proton and electron microprobe study. Chem Geol 117:355–360

Visser W, Koster van Groos AF (1979a) Phase relations in the system K_2O-FeO-Al_2O_3-SiO_2 at 1 atmosphere with special emphasis on low temperature liquid immiscibility. Am J Sci 279:70–91

Visser W, Koster van Groos AK (1979b) Effects of P_2O_5 and TiO_2 on liquid-liquid equilibria in the system K_2O-FeO-Al_2O_3-SiO_2. Am J Sci 279:970–988

Visser WI, Koster van Groos AK (1979c) Effect of pressure on liquid immiscibility in the system K_2O-FeO-Al_2O_3-SiO_2-P_2O_5. Am J Sci 279:1160–1175

Warren BE, Pincus AG (1940) Atomic consideration of immiscibility in glass systems. J Amer Ceram Soc 23(10):301–304

Watson EB (1976) Two-liquid partition coefficients: Experimental data and geochemical implications. Contrib Mineral Petrol 56:119–134

Zhang Y, Ni H, Chen Y (2010) Diffusion data in silicate melts. In: Zhang Y, Cherniak DJ (eds) Diffusion in minerals and melts. De Gruyter, Berlin, pp 311–408